Exhibit 21

SARS-CoV-2 infection induces long-lived bone marrow plasma cells in humans

https://www.nature.com/articles/s41586-021-03647-4

Article

SARS-CoV-2 infection induces long-lived bone marrow plasma cells in humans

https://doi.org/10.1038/s41586-021-03647-4

Received: 20 December 2020

Accepted: 14 May 2021

Published online: 24 May 2021

Check for updates

Jackson S. Turner[1], Wooseob Kim[1], Elizaveta Kalaidina[2], Charles W. Goss[3], Adriana M. Rauseo[4], Aaron J. Schmitz[1], Lena Hansen[1,5], Alem Haile[6], Michael K. Klebert[6], Iskra Pusic[7], Jane A. O'Halloran[4], Rachel M. Presti[4,8] & Ali H. Ellebedy[1,8,9]✉

Long-lived bone marrow plasma cells (BMPCs) are a persistent and essential source of protective antibodies[1–7]. Individuals who have recovered from COVID-19 have a substantially lower risk of reinfection with SARS-CoV-2[8–10]. Nonetheless, it has been reported that levels of anti-SARS-CoV-2 serum antibodies decrease rapidly in the first few months after infection, raising concerns that long-lived BMPCs may not be generated and humoral immunity against SARS-CoV-2 may be short-lived[11–13]. Here we show that in convalescent individuals who had experienced mild SARS-CoV-2 infections ($n = 77$), levels of serum anti-SARS-CoV-2 spike protein (S) antibodies declined rapidly in the first 4 months after infection and then more gradually over the following 7 months, remaining detectable at least 11 months after infection. Anti-S antibody titres correlated with the frequency of S-specific plasma cells in bone marrow aspirates from 18 individuals who had recovered from COVID-19 at 7 to 8 months after infection. S-specific BMPCs were not detected in aspirates from 11 healthy individuals with no history of SARS-CoV-2 infection. We show that S-binding BMPCs are quiescent, which suggests that they are part of a stable compartment. Consistently, circulating resting memory B cells directed against SARS-CoV-2 S were detected in the convalescent individuals. Overall, our results indicate that mild infection with SARS-CoV-2 induces robust antigen-specific, long-lived humoral immune memory in humans.

Reinfections by seasonal coronaviruses occur 6 to 12 months after the previous infection, indicating that protective immunity against these viruses may be short-lived[14,15]. Early reports documenting rapidly declining antibody titres in the first few months after infection in individuals who had recovered from COVID-19 suggested that protective immunity against SARS-CoV-2 might be similarly transient[11–13]. It was also suggested that infection with SARS-CoV-2 could fail to elicit a functional germinal centre response, which would interfere with the generation of long-lived plasma cells[3–5,7,16]. More recent reports analysing samples that were collected approximately 4 to 6 months after infection indicate that SARS-CoV-2 antibody titres decline more slowly than in the initial months after infection[8,17–21]. Durable serum antibody titres are maintained by long-lived plasma cells—non-replicating, antigen-specific plasma cells that are detected in the bone marrow long after the clearance of the antigen[1–7]. We sought to determine whether they were detectable in convalescent individuals approximately 7 months after SARS-CoV-2 infection.

Biphasic decay of anti-S antibody titres

Blood samples were collected approximately 1 month after the onset of symptoms from 77 individuals who were convalescing from COVID-19 (49% female, 51% male, median age 49 years), the majority of whom had experienced mild illness (7.8% hospitalized, Extended Data Tables 1, 2). Follow-up blood samples were collected three times at approximately three-month intervals. Twelve convalescent participants received either the BNT162b2 (Pfizer) or the mRNA-1273 (Moderna) SARS-CoV-2 vaccine between the last two time points; these post-vaccination samples were not included in our analyses. In addition, bone marrow aspirates were collected from 18 of the convalescent individuals at 7 to 8 months after infection and from 11 healthy volunteers with no history of SARS-CoV-2 infection or vaccination. Follow-up bone marrow aspirates were collected from 5 of the 18 convalescent individuals and from 1 additional convalescent donor approximately 11 months after infection (Fig. 1a, Extended Data Tables 3, 4). We first performed a longitudinal analysis of circulating anti-SARS-CoV-2 serum antibodies. Whereas anti-SARS-CoV-2 spike protein (S) IgG antibodies were undetectable in blood from control individuals, 74 out of the 77 convalescent individuals had detectable serum titres approximately 1 month after the onset of symptoms. Between 1 and 4 months after symptom onset, overall anti-S IgG titres decreased from a mean $\log_e$-transformed half-maximal dilution of 6.3 to 5.7 (mean difference 0.59 ± 0.06, $P < 0.001$). However, in the interval between 4 and 11 months after symptom onset, the rate

[1]Department of Pathology and Immunology, Washington University School of Medicine, St Louis, MO, USA. [2]Division of Allergy and Immunology, Department of Internal Medicine, Washington University School of Medicine, St Louis, MO, USA. [3]Division of Biostatistics, Washington University School of Medicine, St Louis, MO, USA. [4]Division of Infectious Diseases, Department of Internal Medicine, Washington University School of Medicine, St Louis, MO, USA. [5]Influenza Centre, Department of Clinical Science, University of Bergen, Bergen, Norway. [6]Clinical Trials Unit, Washington University School of Medicine, St Louis, MO, USA. [7]Division of Oncology, Department of Internal Medicine, Washington University School of Medicine, St Louis, MO, USA. [8]Center for Vaccines and Immunity to Microbial Pathogens, Washington University School of Medicine, St Louis, MO, USA. [9]The Andrew M. and Jane M. Bursky Center for Human Immunology & Immunotherapy Programs, Washington University School of Medicine, St Louis, MO, USA. ✉e-mail: ellebedy@wustl.edu

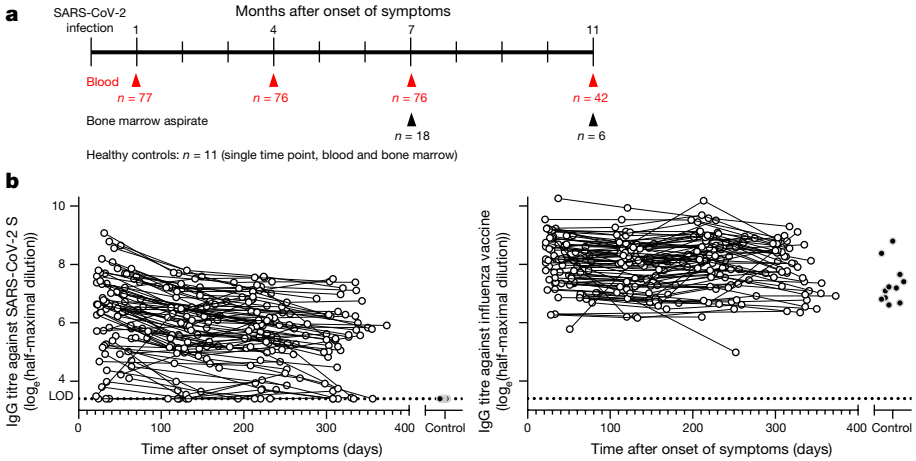

Fig. 1 | SARS-CoV-2 infection elicits durable serum anti-S antibody titres. **a**, Study design. Seventy-seven convalescent individuals who had experienced mild SARS-CoV-2 infections (aged 21–69 years) were enrolled and blood was collected approximately 1 month, 4 months, 7 months and 11 months after the onset of symptoms. Bone marrow aspirates were collected from 18 of the convalescent individuals 7 to 8 months after infection and from 11 healthy volunteers (aged 23–60 years) with no history of SARS-CoV-2 infection. Follow-up bone marrow aspirates were collected from 5 of the 18 convalescent donors and 1 additional convalescent donor approximately 11 months after infection. **b**, Blood IgG titres against SARS-CoV-2 S (left) and influenza virus vaccine (right) measured by enzyme-linked immunosorbent assay (ELISA) in convalescent individuals (white circles) at the indicated time after onset of symptoms, and in control individuals (black circles). The dotted lines indicate the limit of detection (LOD). Mean titres and pairwise differences at each time point were estimated using a linear mixed model analysis.

of decline slowed, and mean titres decreased from 5.7 to 5.3 (mean difference 0.44 ± 0.10, $P < 0.001$; Fig. 1a). In contrast to the anti-S antibody titres, IgG titres against the 2019–2020 inactivated seasonal influenza virus vaccine were detected in all control individuals and individuals who were convalescing from COVID-19, and declined much more gradually, if at all over the course of the study, with mean titres decreasing from 8.0 to 7.9 (mean difference 0.16 ± 0.06, $P = 0.042$) and 7.9 to 7.8 (mean difference 0.02 ± 0.08, $P = 0.997$) across the 1-to-4-month and 4-to-11-month intervals after symptom onset, respectively (Fig. 1b).

Induction of S-binding long-lived BMPCs

The relatively rapid early decline in the levels of anti-S IgG, followed by a slower decrease, is consistent with a transition from serum antibodies being secreted by short-lived plasmablasts to secretion by a smaller but more persistent population of long-lived plasma cells generated later in the immune response. The majority of this latter population resides in the bone marrow[1–6]. To investigate whether individuals who had recovered from COVID-19 developed a virus-specific long-lived BMPC compartment, we examined bone marrow aspirates obtained approximately 7 and 11 months after infection for anti-SARS-CoV-2 S-specific BMPCs. We magnetically enriched BMPCs from the aspirates and then quantified the frequencies of those secreting IgG and IgA directed against the 2019–2020 influenza virus vaccine, the tetanus–diphtheria vaccine and SARS-CoV-2 S by enzyme-linked immunosorbent spot assay (ELISpot) (Fig. 2a). Frequencies of influenza- and tetanus–diphtheria-vaccine-specific BMPCs were comparable between control individuals and convalescent individuals. IgG- and IgA-secreting S-specific BMPCs were detected in 15 and 9 of the 19 convalescent individuals, respectively, but not in any of the 11 control individuals (Fig. 2b). Notably, none of the control individuals or convalescent individuals had detectable S-specific antibody-secreting cells in the blood at the time of bone marrow sampling, indicating that the detected BMPCs represent bone-marrow-resident cells and not contamination from circulating plasmablasts. Frequencies of anti-S IgG BMPCs were stable among the 5 convalescent individuals who were sampled a second time approximately 4 months later, and frequencies of anti-S IgA BMPCs were stable in 4 of these 5 individuals but had decreased to below the limit of detection in one individual (Fig. 2c). Consistent with their stable BMPC frequencies, anti-S IgG titres in the 5 convalescent individuals remained consistent between 7 and 11 months after symptom onset. IgG titres measured against the receptor-binding domain (RBD) of the S protein—a primary target of neutralizing antibodies—were detected in 4 of the 5 convalescent individuals and were also stable between 7 and 11 months after symptom onset (Fig. 2d). Frequencies of anti-S IgG BMPCs showed a modest but significant correlation with circulating anti-S IgG titres at 7–8 months after the onset of symptoms in convalescent individuals, consistent with the long-term maintenance of antibody levels by these cells ($r = 0.48$, $P = 0.046$). In accordance with previous reports[22–24], frequencies of influenza-vaccine-specific IgG BMPCs and antibody titres exhibited a strong and significant correlation ($r = 0.67$, $P < 0.001$; Fig. 2e). Nine of the aspirates from control individuals and 12 of the 18 aspirates that were collected 7 months after symptom onset from convalescent individuals yielded a sufficient number of BMPCs for additional analysis by flow cytometry. We stained these samples intracellularly with fluorescently labelled S and influenza virus haemagglutinin (HA) probes to identify and characterize antigen-specific BMPCs. As controls, we also intracellularly stained peripheral blood mononuclear cells (PBMCs) from healthy volunteers one week after vaccination against SARS-CoV-2 or seasonal influenza virus (Fig. 3a, Extended Data Fig. 1a–c). Consistent with the ELISpot data, low frequencies of S-binding BMPCs were detected in 10 of the 12 samples from convalescent individuals, but not in any of the 9 control samples (Fig. 3b). Although both recently generated circulating plasmablasts and S- and HA-binding BMPCs expressed BLIMP-1, the BMPCs were differentiated by their lack of expression of Ki-67—indicating a quiescent state—as well as by higher levels of CD38 (Fig. 3c).

Robust S-binding memory B cell response

Memory B cells form the second arm of humoral immune memory. After re-exposure to an antigen, memory B cells rapidly expand and differentiate into antibody-secreting plasmablasts. We examined the frequency of SARS-CoV-2-specific circulating memory B cells in individuals who were convalescing from COVID-19 and in healthy control individuals. We stained PBMCs with fluorescently labelled S probes and determined the frequency of S-binding memory B cells among isotype-switched $IgD^{lo}CD20^{+}$ memory B cells by flow cytometry. For comparison, we

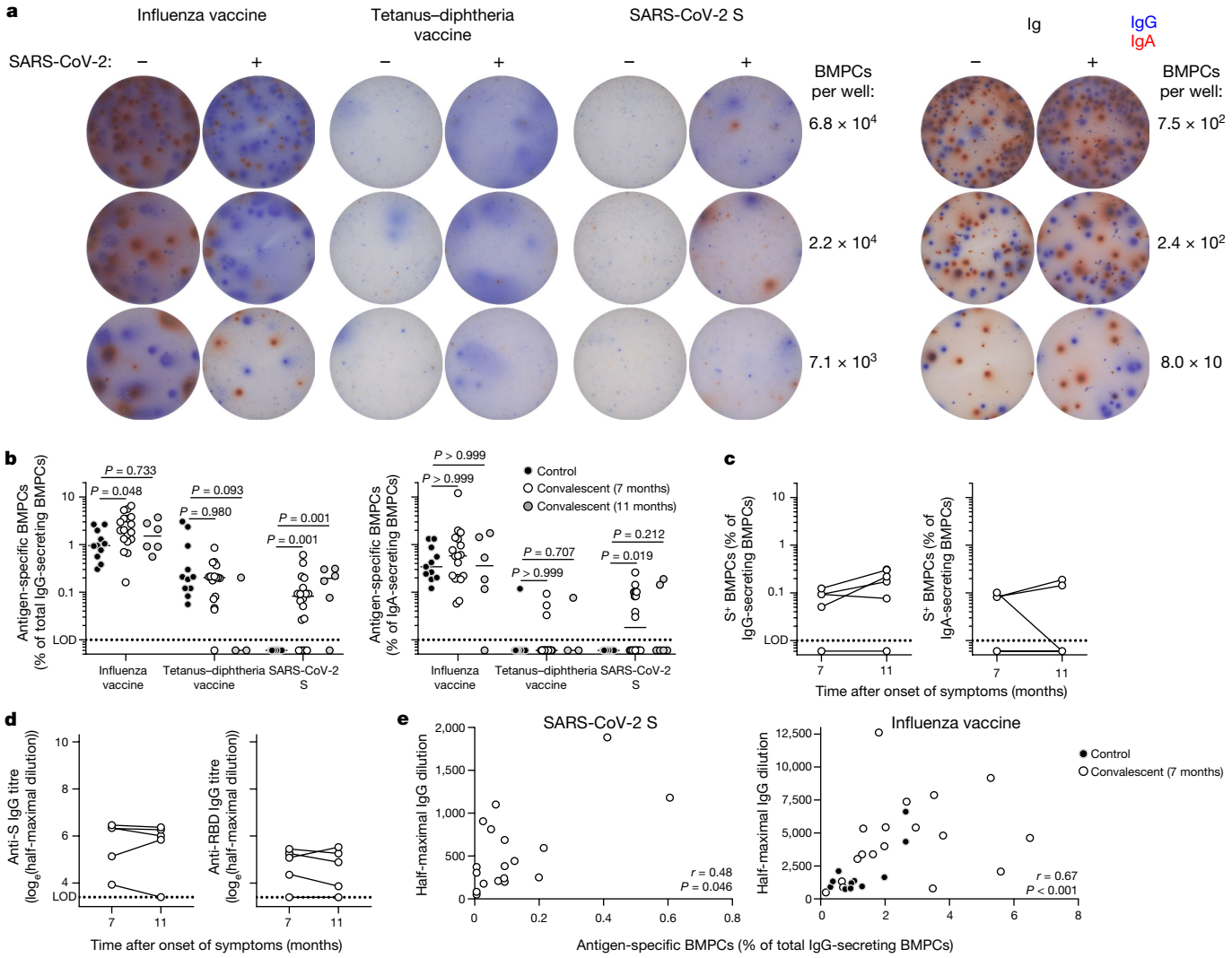

Fig. 2 | SARS-CoV-2 infection elicits S-binding long-lived BMPCs. **a**, Representative images of ELISpot wells coated with the indicated antigens or anti-immunoglobulin (Ig) and developed in blue and red for IgG and IgA, respectively, after incubation of magnetically enriched BMPCs from control individuals and convalescent individuals. **b**, Frequencies of BMPCs secreting IgG (left) or IgA (right) antibodies specific for the indicated antigens, indicated as percentages of total IgG- or IgA-secreting BMPCs in control individuals (black circles) or convalescent individuals 7 months (white circles) or 11 months (grey circles) after symptom onset. Horizontal lines indicate the median. *P* values from two-sided Kruskal–Wallis tests with Dunn's correction for multiple comparisons between control individuals and convalescent individuals. Each symbol represents one sample ($n = 18$ convalescent, $n = 11$ control). **c**, Paired frequencies of S-binding BMPCs among IgG-secreting (left) and IgA-secreting (right) BMPCs from convalescent individuals 7 months and 11 months after symptom onset. **d**, Paired anti-S (left) and anti-RBD (right) IgG serum antibody titres from convalescent individuals 7 months and 11 months after symptom onset. Data in **c** and **d** (left) are also shown in **b** and Fig. 1b, respectively. Each symbol represents one sample ($n = 5$). Dotted lines indicate the limit of detection. **e**, Frequencies of BMPCs secreting IgG antibodies specific for SARS-CoV-2 S (left) and influenza virus vaccine (right) plotted against respective IgG titres in paired blood samples from control individuals (black circles) or convalescent individuals 7 months after symptom onset (white circles). *P* and *r* values from two-sided Spearman's correlations. Each symbol represents one sample ($n = 18$ convalescent, $n = 11$ control).

co-stained the cells with fluorescently labelled influenza virus HA probes (Fig. 4a, Extended Data Fig. 1d). S-binding memory B cells were identified in convalescent individuals in the first sample that was collected approximately one month after the onset of symptoms, with comparable frequencies to influenza HA-binding memory B cells (Fig. 4b). S-binding memory B cells were maintained for at least 7 months after symptom onset and were present at significantly higher frequencies relative to healthy controls—comparable to the frequencies of influenza HA-binding memory B cells that were identified in both groups (Fig. 4c).

Discussion

This study sought to determine whether infection with SARS-CoV-2 induces antigen-specific long-lived BMPCs in humans. We detected SARS-CoV-2 S-specific BMPCs in bone marrow aspirates from 15 out of 19 convalescent individuals, and in none from the 11 control participants. The frequencies of anti-S IgG BMPCs modestly correlated with serum IgG titres at 7–8 months after infection. Phenotypic analysis by flow cytometry showed that S-binding BMPCs were quiescent, and their frequencies were largely consistent in 5 paired aspirates collected at 7 and 11 months after symptom onset. Notably, we detected no S-binding cells among plasmablasts in blood samples collected at the same time as the bone marrow aspirates by ELISpot or flow cytometry in any of the convalescent or control samples. Together, these data indicate that mild SARS-CoV-2 infection induces a long-lived BMPC response. In addition, we showed that S-binding memory B cells in the blood of individuals who had recovered from COVID-19 were present at similar frequencies to those directed against influenza virus HA. Overall, our

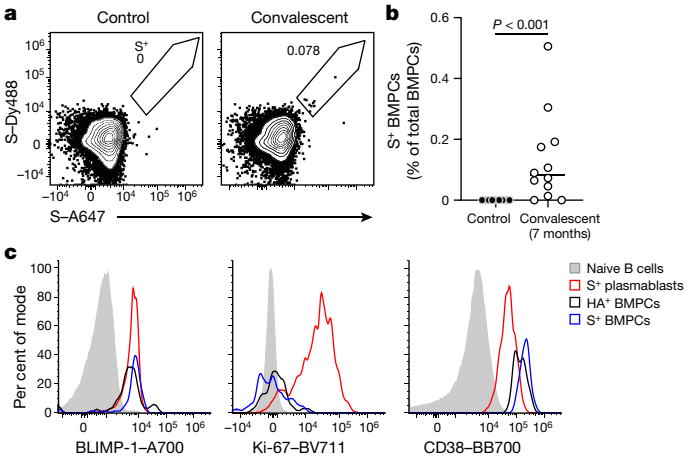

Fig. 3 | SARS-CoV-2 S-binding BMPCs are quiescent and distinct from circulating plasmablasts. a, Representative plots of intracellular S staining in $CD20^{lo}CD38^{+}IgD^{lo}CD19^{+/lo}CD3^{-}$ live singlet BMPCs (gating in Extended Data Fig. 1a) from magnetically enriched BMPCs from control individuals (left) or convalescent individuals 7 months after symptom onset (right). **b**, Frequencies of S-binding BMPCs in total BMPCs from control individuals (black circles) or convalescent individuals 7 months after symptom onset (white circles). Horizontal lines indicate the median. *P* value from two-sided Mann–Whitney *U* test. Each symbol represents one sample ($n = 12$ convalescent, $n = 9$ control). **c**, Histograms of BLIMP-1 (left), Ki-67 (centre), and CD38 (right) staining in S^{+} (blue) and HA^{+} (black) BMPCs from magnetically enriched BMPCs 7 months after symptom onset, and in S^{+} plasmablasts (red) and naive B cells (grey) from healthy donor PBMCs 1 week after SARS-CoV-2 S immunization.

results are consistent with SARS-CoV-2 infection eliciting a canonical T-cell-dependent B cell response, in which an early transient burst of extrafollicular plasmablasts generates a wave of serum antibodies that decline relatively quickly. This is followed by more stably maintained levels of serum antibodies that are supported by long-lived BMPCs.

Although this overall trend captures the serum antibody dynamics of the majority of participants, we observed that in three participants, anti-S serum antibody titres increased between 4 and 7 months after the onset of symptoms, after having initially declined between 1 and 4 months. This could be stochastic noise, could represent increased net binding affinity as early plasmablast-derived antibodies are replaced by those from affinity-matured BMPCs, or could represent increases in antibody concentration from re-encounter with the virus (although none of the participants in our cohort tested positive a second time). Although anti-S IgG titres in the convalescent cohort were relatively stable in the interval between 4 and 11 months after symptom onset, they did measurably decrease, in contrast to anti-influenza virus vaccine titres. It is possible that this decline reflects a final waning of early plasmablast-derived antibodies. It is also possible that the lack of decline in influenza titres was due to boosting through exposure to influenza antigens. Our data suggest that SARS-CoV-2 infection induces a germinal centre response in humans because long-lived BMPCs are thought to be predominantly germinal-centre-derived[7]. This is consistent with a recent study that reported increased levels of somatic hypermutation in memory B cells that target the RBD of SARS-CoV-2 S in convalescent individuals at 6 months compared to 1 month after infection[20].

To our knowledge, the current study provides the first direct evidence for the induction of antigen-specific BMPCs after a viral infection in humans. However, we do acknowledge several limitations. Although we detected anti-S IgG antibodies in serum at least 7 months after infection in all 19 of the convalescent donors from whom we obtained bone marrow aspirates, we failed to detect S-specific BMPCs in 4 donors. Serum anti-S antibody titres in those four donors were low, suggesting that S-specific BMPCs may potentially be present at very low frequencies that are below the limit of detection of the assay. Another limitation is that we do not know the fraction of the S-binding BMPCs detected in our study that encodes neutralizing antibodies. SARS-CoV-2 S protein is the main target of neutralizing antibodies[17,25–30] and a correlation between serum anti-S IgG binding and neutralization titres has been documented[17,31]. Further studies will be required to determine the

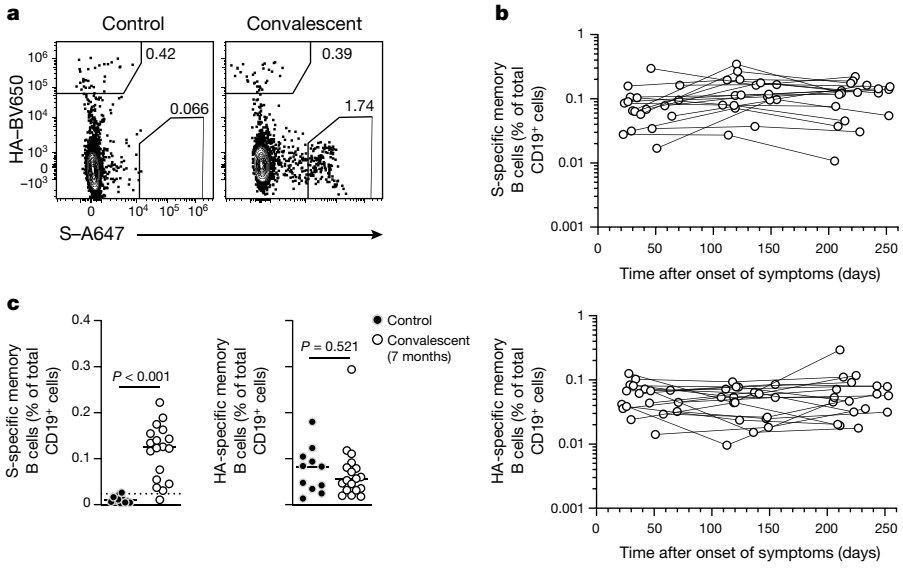

Fig. 4 | SARS-CoV-2 infection elicits a robust memory B cell response. a, Representative plots of surface influenza virus HA and S staining in $CD20^{+}CD38^{lo/int}IgD^{lo}CD19^{+}CD3^{-}$ live singlet memory B cells (gating in Extended Data Fig. 1d) from PBMCs from control individuals (left) and convalescent individuals 7 months after symptom onset (right). **b**, Kinetics of S- (top) and HA- (bottom) binding memory B cells in PBMCs from convalescent individuals, collected at the indicated days after symptom onset. Data from the 7-month time point are also shown in **c**. **c**, Frequencies of S- (left) and HA- (right) binding memory B cells in PBMCs from control individuals (black circles) and convalescent individuals 7 months after symptom onset (white circles). The dotted line in the left plot indicates the limit of sensitivity, which was defined as the median + 2× s.d. of the controls. Each symbol represents one sample ($n = 18$ convalescent, $n = 11$ control). Horizontal lines indicate the median. *P* values from two-sided Mann–Whitney *U* tests.

epitopes that are targeted by BMPCs and memory B cells, as well as their clonal relatedness. Finally, although our data document a robust induction of long-lived BMPCs after infection with SARS-CoV-2, it is critical to note that our convalescent individuals mostly experienced mild infections. Our data are consistent with a report showing that individuals who recovered rapidly from symptomatic SARS-CoV-2 infection generated a robust humoral immune response[32]. It is possible that more-severe SARS-CoV-2 infections could lead to a different outcome with respect to long-lived BMPC frequencies, owing to dysregulated humoral immune responses. This, however, has not been the case in survivors of the 2014 Ebola virus outbreak in West Africa, in whom severe viral infection induced long-lasting antigen-specific serum IgG antibodies[33].

Long-lived BMPCs provide the host with a persistent source of preformed protective antibodies and are therefore needed to maintain durable immune protection. However, the longevity of serum anti-S IgG antibodies is not the only determinant of how durable immune-mediated protection will be. Isotype-switched memory B cells can rapidly differentiate into antibody-secreting cells after re-exposure to a pathogen, offering a second line of defence[34]. Encouragingly, the frequency of S-binding circulating memory B cells at 7 months after infection was similar to that of B cells directed against contemporary influenza HA antigens. Overall, our data provide strong evidence that SARS-CoV-2 infection in humans robustly establishes the two arms of humoral immune memory: long-lived BMPCs and memory B cells. These findings provide an immunogenicity benchmark for SARS-CoV-2 vaccines and a foundation for assessing the durability of primary humoral immune responses that are induced in humans after viral infections.

Online content

Any methods, additional references, Nature Research reporting summaries, source data, extended data, supplementary information, acknowledgements, peer review information; details of author contributions and competing interests; and statements of data and code availability are available at https://doi.org/10.1038/s41586-021-03647-4.

1. Benner, R., Meima, F., van der Meulen, G. M. & van Muiswinkel, W. B. Antibody formation in mouse bone marrow. I. Evidence for the development of plaque-forming cells in situ. *Immunology* **26**, 247–255 (1974).
2. Manz, R. A., Thiel, A. & Radbruch, A. Lifetime of plasma cells in the bone marrow. *Nature* **388**, 133–134 (1997).
3. Slifka, M. K., Antia, R., Whitmire, J. K. & Ahmed, R. Humoral immunity due to long-lived plasma cells. *Immunity* **8**, 363–372 (1998).
4. Hammarlund, E. et al. Duration of antiviral immunity after smallpox vaccination. *Nat. Med.* **9**, 1131–1137 (2003).
5. Halliley, J. L. et al. Long-lived plasma cells are contained within the $CD19^{-}CD38^{hi}CD138^{+}$ subset in human bone marrow. *Immunity* **43**, 132–145 (2015).
6. Mei, H. E. et al. A unique population of IgG-expressing plasma cells lacking CD19 is enriched in human bone marrow. *Blood* **125**, 1739–1748 (2015).
7. Nutt, S. L., Hodgkin, P. D., Tarlinton, D. M. & Corcoran, L. M. The generation of antibody-secreting plasma cells. *Nat. Rev. Immunol.* **15**, 160–171 (2015).
8. Hall, V. J. et al. SARS-CoV-2 infection rates of antibody-positive compared with antibody-negative health-care workers in England: a large, multicentre, prospective cohort study (SIREN). *Lancet* **397**, 1459–1469 (2021).
9. Houlihan, C. F. et al. Pandemic peak SARS-CoV-2 infection and seroconversion rates in London frontline health-care workers. *Lancet* **396**, e6–e7 (2020).
10. Lumley, S. F. et al. Antibodies to SARS-CoV-2 are associated with protection against reinfection. Preprint at https://doi.org/10.1101/2020.11.18.20234369 (2020).
11. Long, Q.-X. et al. Clinical and immunological assessment of asymptomatic SARS-CoV-2 infections. *Nat. Med.* **26**, 1200–1204 (2020).
12. Ibarrondo, F. J. et al. Rapid decay of anti-SARS-CoV-2 antibodies in persons with mild Covid-19. *N. Engl. J. Med.* **383**, 1085–1087 (2020).
13. Seow, J. et al. Longitudinal observation and decline of neutralizing antibody responses in the three months following SARS-CoV-2 infection in humans. *Nat. Microbiol.* **5**, 1598–1607 (2020).
14. Edridge, A. W. D. et al. Seasonal coronavirus protective immunity is short-lasting. *Nat. Med.* **26**, 1691–1693 (2020).
15. Callow, K. A., Parry, H. F., Sergeant, M. & Tyrrell, D. A. The time course of the immune response to experimental coronavirus infection of man. *Epidemiol. Infect.* **105**, 435–446 (1990).
16. Kaneko, N. et al. Loss of Bcl-6-expressing T follicular helper cells and germinal centers in COVID-19. *Cell* **183**, 143–157 (2020).
17. Wajnberg, A. et al. Robust neutralizing antibodies to SARS-CoV-2 infection persist for months. *Science* **370**, 1227–1230 (2020).
18. Isho, B. et al. Persistence of serum and saliva antibody responses to SARS-CoV-2 spike antigens in COVID-19 patients. *Sci. Immunol.* **5**, eabe5511 (2020).
19. Dan, J. M. et al. Immunological memory to SARS-CoV-2 assessed for up to 8 months after infection. *Science* **371**, eabf4063 (2021).
20. Gaebler, C. et al. Evolution of antibody immunity to SARS-CoV-2. *Nature* **591**, 639–644 (2021).
21. Rodda, L. B. et al. Functional SARS-CoV-2-specific immune memory persists after mild COVID-19. *Cell* **184**, 169–183 (2021).
22. Davis, C. W. et al. Influenza vaccine-induced human bone marrow plasma cells decline within a year after vaccination. *Science* **370**, 237–241 (2020).
23. Turesson, I. Distribution of immunoglobulin-containing cells in human bone marrow and lymphoid tissues. *Acta Med. Scand.* **199**, 293–304 (1976).
24. Pritz, T. et al. Plasma cell numbers decrease in bone marrow of old patients. *Eur. J. Immunol.* **45**, 738–746 (2015).
25. Shi, R. et al. A human neutralizing antibody targets the receptor-binding site of SARS-CoV-2. *Nature* **584**, 120–124 (2020).
26. Cao, Y. et al. Potent neutralizing antibodies against SARS-CoV-2 identified by high-throughput single-cell sequencing of convalescent patients' B cells. *Cell* **182**, 73–84 (2020).
27. Robbiani, D. F. et al. Convergent antibody responses to SARS-CoV-2 in convalescent individuals. *Nature* **584**, 437–442 (2020).
28. Kreer, C. et al. Longitudinal isolation of potent near-germline SARS-CoV-2-neutralizing antibodies from COVID-19 patients. *Cell* **182**, 843–854 (2020).
29. Alsoussi, W. B. et al. A potently neutralizing antibody protects mice against SARS-CoV-2 infection. *J. Immunol.* **205**, 915–922 (2020).
30. Wang, C. et al. A human monoclonal antibody blocking SARS-CoV-2 infection. *Nat. Commun.* **11**, 2251 (2020).
31. Wang, K. et al. Longitudinal dynamics of the neutralizing antibody response to severe acute respiratory syndrome coronavirus 2 (SARS-CoV-2) Infection. *Clin. Infect. Dis.* **2020**, ciaa1143 (2020).
32. Chen, Y. et al. Quick COVID-19 healers sustain anti-SARS-CoV-2 antibody production. *Cell* **183**, 1496–1507 (2020).
33. Davis, C. W. et al. Longitudinal analysis of the human B Cell response to ebola virus infection. *Cell* **177**, 1566–1582 (2019).
34. Ellebedy, A. H. et al. Defining antigen-specific plasmablast and memory B cell subsets in human blood after viral infection or vaccination. *Nat. Immunol.* **17**, 1226–1234 (2016).

Methods

Data reporting

No statistical methods were used to predetermine sample size. The experiments were not randomized and the investigators were not blinded during outcome assessment.

Sample collection, preparation and storage

All studies were approved by the Institutional Review Board of Washington University in St Louis. Written consent was obtained from all participants. Seventy-seven participants who had recovered from SARS-CoV-2 infection and eleven control individuals without a history of SARS-CoV-2 infection were enrolled (Extended Data Tables 1, 4). Blood samples were collected in EDTA tubes and PBMCs were enriched by density gradient centrifugation over Ficoll 1077 (GE) or Lymphopure (BioLegend). The remaining red blood cells were lysed with ammonium chloride lysis buffer, and cells were immediately used or cryopreserved in 10% dimethyl sulfoxide in fetal bovine serum (FBS). Bone marrow aspirates of approximately 30 ml were collected in EDTA tubes from the iliac crest of 18 individuals who had recovered from COVID-19 and the control individuals. Bone marrow mononuclear cells were enriched by density gradient centrifugation over Ficoll 1077, and the remaining red blood cells were lysed with ammonium chloride buffer (Lonza) and washed with phosphate-buffered saline (PBS) supplemented with 2% FBS and 2 mM EDTA. Bone marrow plasma cells were enriched from bone marrow mononuclear cells using the CD138 Positive Selection Kit II (Stemcell) and immediately used for ELISpot or cryopreserved in 10% dimethyl sulfoxide in FBS.

Antigens

Recombinant soluble spike protein (S) and its receptor-binding domain (RBD) derived from SARS-CoV-2 were expressed as previously described[35]. In brief, mammalian cell codon-optimized nucleotide sequences coding for the soluble version of S (GenBank: MN908947.3, amino acids (aa) 1–1,213) including a C-terminal thrombin cleavage site, T4 foldon trimerization domain and hexahistidine tag cloned into the mammalian expression vector pCAGGS. The S protein sequence was modified to remove the polybasic cleavage site (RRAR to A) and two stabilizing mutations were introduced (K986P and V987P, wild-type numbering). The RBD, along with the signal peptide (aa 1–14) plus a hexahistidine tag were cloned into the mammalian expression vector pCAGGS. Recombinant proteins were produced in Expi293F cells (Thermo Fisher Scientific) by transfection with purified DNA using the ExpiFectamine 293 Transfection Kit (Thermo Fisher Scientific). Supernatants from transfected cells were collected 3 (for S) or 4 (for RBD) days after transfection, and recombinant proteins were purified using Ni-NTA agarose (Thermo Fisher Scientific), then buffer-exchanged into PBS and concentrated using Amicon Ultracel centrifugal filters (EMD Millipore). For flow cytometry staining, recombinant S was labelled with Alexa Fluor 647- or DyLight 488-NHS ester (Thermo Fisher Scientific); excess Alexa Fluor 647 and DyLight 488 were removed using 7-kDa and 40-kDa Zeba desalting columns, respectively (Pierce). Recombinant HA from A/Michigan/45/2015 (aa 18–529, Immune Technology) was labelled with DyLight 405-NHS ester (Thermo Fisher Scientific); excess DyLight 405 was removed using 7-kDa Zeba desalting columns. Recombinant HA from A/Brisbane/02/2018 (aa 18–529) and B/Colorado/06/2017 (aa 18–546) (both Immune Technology) were biotinylated using the EZ-Link Micro NHS-PEG4-Biotinylation Kit (Thermo Fisher Scientific); excess biotin was removed using 7-kDa Zeba desalting columns.

ELISpot

Plates were coated with Flucelvax Quadrivalent 2019/2020 seasonal influenza virus vaccine (Sequiris), tetanus–diphtheria vaccine (Grifols), recombinant S or anti-human Ig. Direct ex vivo ELISpot was performed to determine the number of total, vaccine-binding or recombinant S-binding IgG- and IgA-secreting cells present in BMPC and PBMC samples using IgG/IgA double-colour ELISpot Kits (Cellular Technology) according to the manufacturer's instructions. ELISpot plates were analysed using an ELISpot counter (Cellular Technology).

ELISA

Assays were performed in 96-well plates (MaxiSorp, Thermo Fisher Scientific) coated with 100 µl of Flucelvax 2019/2020 or recombinant S in PBS, and plates were incubated at 4 °C overnight. Plates were then blocked with 10% FBS and 0.05% Tween-20 in PBS. Serum or plasma were serially diluted in blocking buffer and added to the plates. Plates were incubated for 90 min at room temperature and then washed 3 times with 0.05% Tween-20 in PBS. Goat anti-human IgG–HRP (Jackson ImmunoResearch, 1:2,500) was diluted in blocking buffer before adding to wells and incubating for 60 min at room temperature. Plates were washed 3 times with 0.05% Tween-20 in PBS, and then washed 3 times with PBS before the addition of *o*-phenylenediamine dihydrochloride peroxidase substrate (Sigma-Aldrich). Reactions were stopped by the addition of 1 M HCl. Optical density measurements were taken at 490 nm. The half-maximal binding dilution for each serum or plasma sample was calculated using nonlinear regression (GraphPad Prism v.8). The limit of detection was defined as 1:30.

Statistics

Spearman's correlation coefficients were estimated to assess the relationship between 7-month anti-S and anti-influenza virus vaccine IgG titres and the frequencies of BMPCs secreting IgG specific for S and for influenza virus vaccine, respectively. Means and pairwise differences of antibody titres at each time point were estimated using a linear mixed model analysis with a first-order autoregressive covariance structure. Time since symptom onset was treated as a categorical fixed effect for the 4 different sample time points spaced approximately 3 months apart. *P* values were adjusted for multiple comparisons using Tukey's method. All analyses were conducted using SAS v.9.4 (SAS Institute) and Prism v.8.4 (GraphPad), and *P* values of less than 0.05 were considered significant.

Flow cytometry

Staining for flow cytometry analysis was performed using cryo-preserved magnetically enriched BMPCs and cryo-preserved PBMCs. For BMPC staining, cells were stained for 30 min on ice with CD45-A532 (HI30, Thermo Fisher Scientific, 1:50), CD38-BB700 (HIT2, BD Horizon, 1:500), CD19-PE (HIB19, 1:200), CXCR5-PE-Dazzle 594 (J252D4, 1:50), CD71-PE-Cy7 (CY1G4, 1:400), CD20-APC-Fire750 (2H7, 1:400), CD3-APC-Fire810 (SK7, 1:50) and Zombie Aqua (all BioLegend) diluted in Brilliant Stain buffer (BD Horizon). Cells were washed twice with 2% FBS and 2 mM EDTA in PBS (P2), fixed for 1 h using the True Nuclear permeabilization kit (BioLegend), washed twice with perm/wash buffer, stained for 1h with DyLight 405-conjugated recombinant HA from A/Michigan/45/2015, DyLight 488- and Alexa 647-conjugated S, Ki-67-BV711 (Ki-67, 1:200, BioLegend) and BLIMP-1-A700 (646702, 1:50, R&D), washed twice with perm/wash buffer, and resuspended in P2. For memory B cell staining, PBMCs were stained for 30 min on ice with biotinylated recombinant HAs diluted in P2, washed twice, then stained for 30 min on ice with Alexa 647-conjugated S, IgA-FITC (M24A, Millipore, 1:500), IgG-BV480 (goat polyclonal, Jackson ImmunoResearch, 1:100), IgD-SB702 (IA6-2, Thermo Fisher Scientific, 1:50), CD38-BB700 (HIT2, BD Horizon, 1:500), CD20-Pacific Blue (2H7, 1:400), CD4-BV570 (OKT4, 1:50), CD24-BV605 (ML5, 1:100), streptavidin-BV650, CD19-BV750 (HIB19, 1:100), CD71-PE (CY1G4, 1:400), CXCR5-PE-Dazzle 594 (J252D4, 1:50), CD27-PE-Cy7 (O323, 1:200), IgM-APC-Fire750 (MHM-88, 1:100), CD3-APC-Fire810 (SK7, 1:50) and Zombie NIR (all BioLegend) diluted in Brilliant Stain buffer (BD Horizon), and washed twice with P2. Cells were acquired on an Aurora using SpectroFlo v.2.2 (Cytek). Flow cytometry data were analysed using FlowJo v.10 (Treestar). In each experiment,

PBMCs were included from convalescent individuals and control individuals.

Reporting summary

Further information on research design is available in the Nature Research Reporting Summary linked to this paper.

Data availability

Relevant data are available from the corresponding author upon reasonable request.

35. Stadlbauer, D. et al. SARS-CoV-2 seroconversion in humans: a detailed protocol for a serological assay, antigen production, and test setup. *Curr. Protoc. Microbiol.* **57**, e100 (2020).

Acknowledgements We thank the donors for providing specimens; T. Lei for assistance with preparing specimens; and L. Kessels, A. J. Winingham, the staff of the Infectious Diseases Clinical Research Unit at Washington University School of Medicine and the nursing team of the bone marrow biopsy suite at Washington University School of Medicine and Barnes Jewish Hospital for sample collection and providing care for donors. The SARS-CoV-2 S and RBD protein expression plasmids were provided by F. Krammer. The Ellebedy laboratory was supported by National Institute of Allergy and Infectious Diseases (NIAID) grants U01AI141990 and 1U01AI150747, NIAID Centers of Excellence for Influenza Research and Surveillance contracts HHSN272201400006C and HHSN272201400008C and NIAID Collaborative Influenza Vaccine Innovation Centers contract 75N93019C00051. J.S.T. was supported by NIAID 5T32CA009547. L.H. was supported by Norwegian Research Council grant 271160 and National Graduate School in Infection Biology and Antimicrobials grant 249062. This study used samples obtained from the Washington University School of Medicine's COVID-19 biorepository, which is supported by the NIH–National Center for Advancing Translational Sciences grant UL1 TR002345. The content is solely the responsibility of the authors and does not necessarily represent the view of the NIH. The WU353, WU367 and WU368 studies were reviewed and approved by the Washington University Institutional Review Board (approval nos. 202003186, 202009100 and 202012081, respectively).

Author contributions A.H.E. conceived and designed the study. J.S.T. and A.H.E. designed experiments and composed the manuscript. A.H., M.K.K., I.P., J.A.O. and R.M.P. wrote and maintained the Institutional Review Board protocol, recruited and phlebotomized participants and coordinated sample collection. J.S.T., W.K., E.K., A.J.S. and L.H. processed specimens. A.J.S. expressed S and RBD proteins. J.S.T., W.K. and E.K. performed ELISA and ELISpot. J.S.T. performed flow cytometry. J.S.T., A.M.R., C.W.G. and A.H.E. analysed data. All authors reviewed the manuscript.

Competing interests The Ellebedy laboratory received funding under sponsored research agreements that are unrelated to the data presented in the current study from Emergent BioSolutions and from AbbVie. J.S.T., A.J.S. and A.H.E. are recipients of a licensing agreement with Abbvie that is unrelated to the data presented in the current study. A.H.E. is a consultant for Mubadala Investment Company and the founder of ImmuneBio Consulting. All other authors declare no competing interests.

Additional information

Supplementary information The online version contains supplementary material available at https://doi.org/10.1038/s41586-021-03647-4.

Correspondence and requests for materials should be addressed to A.H.E.

Peer review information *Nature* thanks Stanley Perlman, Andreas Radbruch and the other, anonymous, reviewer(s) for their contribution to the peer review of this work. Peer reviewer reports are available.

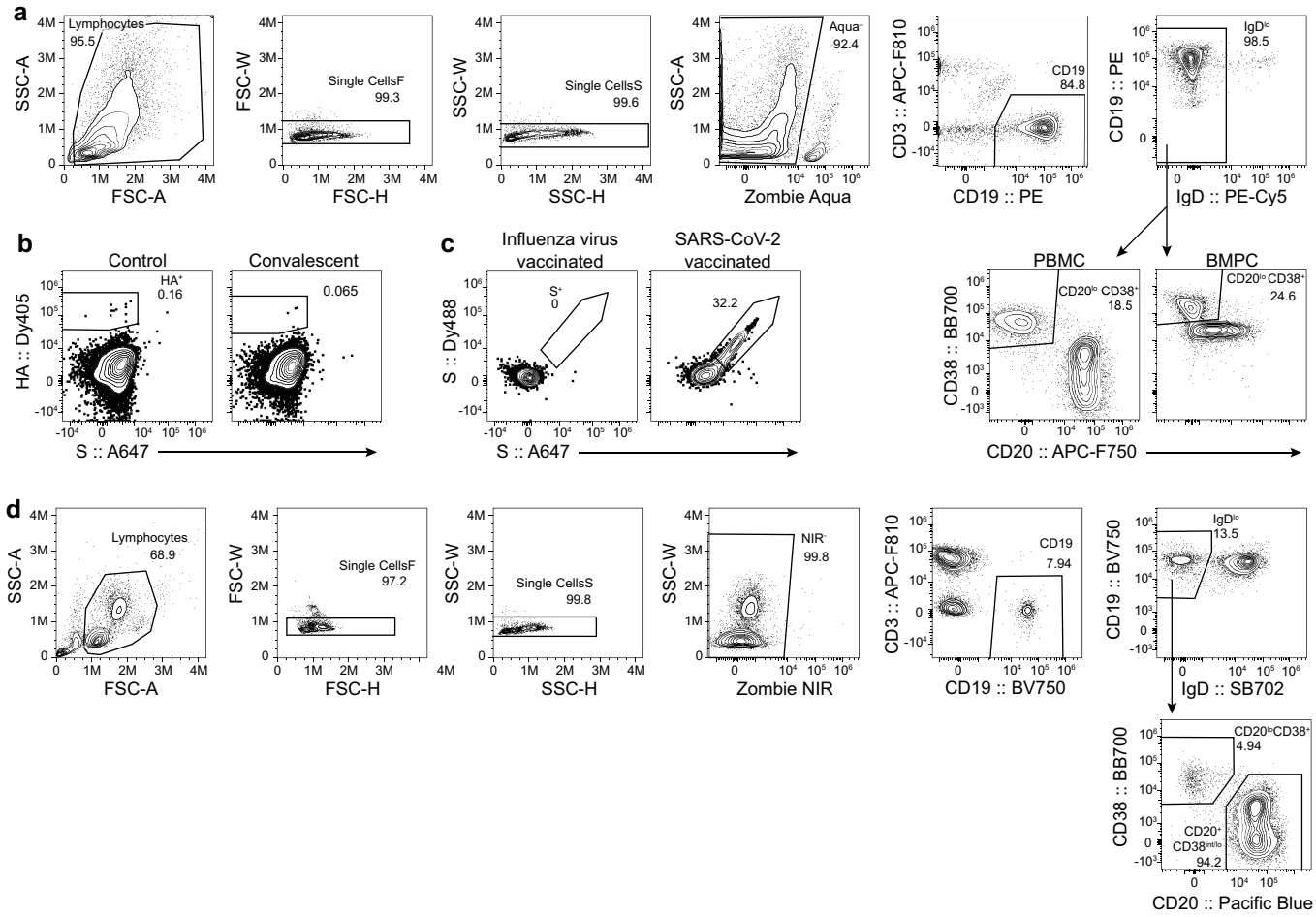

Extended Data Fig. 1 | Flow cytometry identification of SARS-CoV-2-elicited plasma cells and memory B cells. a, **d**, Flow cytometry gating strategies for BMPCs in magnetically enriched BMPCs and plasmablasts in PBMCs (**a**) and isotype-switched memory B cells and plasmablasts in PBMCs (**d**). **b**, Representative plots of intracellular SARS-CoV-2 S and influenza virus HA staining in BMPCs from samples from control individuals (left) and individuals who were convalescing from COVID-19 (right) 7 months after symptom onset. **c**, Representative plots of intracellular S staining in plasmablasts in PBMCs one week after vaccination against seasonal influenza virus or SARS-CoV-2.

Extended Data Table 1 | Demographics of patients with COVID-19

	Total N=77 N (%)	Bone marrow biopsy N=19 N (%)
Age (median [range])	49 (21-69)	52 (30-69)
Sex		
Female	38 (49.4)	7 (36.8)
Male	39 (50.6)	12 (63.2)
Race		
White	70 (90.9)	18 (94.7)
Black	1 (1.3)	0 (0)
Asian	4 (5.2)	0 (0)
Other	2 (2.6)	1 (5.3)
Comorbidities		
Asthma	13 (16.9)	3 (15.8)
Lung disease	0 (0)	0 (0)
Heart disease	3 (3.9)	0 (0)
Hypertension	13 (16.9)	6 (31.6)
Diabetes mellitus	3 (3.9)	3 (15.8)
Cancer	10 (13)	3 (15.8)
Autoimmune disease	4 (5.2)	2 (10.5)
Hyperlipidemia	8 (10.4)	2 (10.5)
Hypothyroidism	5 (6.5)	3 (15.8)
Gastroesophageal reflux disease	5 (6.5)	2 (10.5)
Other	26 (33.8)	10 (52.6)
Solid organ transplant	1 (1.3)	1 (5.3)
Obesity	1 (1.3)	0 (0)

Extended Data Table 2 | Symptoms of patients with COVID-19

	Total N=77 N (%)	Bone marrow biopsy N=19 N (%)
First symptom		
Cough	12 (15.6)	3 (15.8)
Diarrhea	1 (1.3)	0 (0)
Dyspnea	2 (2.6)	1 (5.3)
Fatigue	7 (9.1)	0 (0)
Fever	22 (28.6)	9 (47.4)
Headache	8 (10.4)	2 (10.5)
Loss of taste	3 (3.9)	2 (10.5)
Malaise	4 (5.2)	1 (5.3)
Myalgias	9 (11.7)	0 (0)
Nasal congestion	2 (2.6)	0 (0)
Nausea	1 (1.3)	0 (0)
Night sweats	1 (1.3)	0 (0)
Sore throat	5 (6.5)	1 (5.3)
Symptom present during disease		
Fever	65 (84.4)	17 (89.5)
Cough	54 (70.1)	14 (73.7)
Dyspnea	31 (40.3)	11 (57.9)
Nausea	19 (24.7)	4 (21.1)
Vomiting	9 (11.7)	3 (15.8)
Diarrhea	39 (50.6)	10 (52.6)
Headaches	47 (61)	12 (63.2)
Loss of taste	42 (54.5)	11 (57.9)
Loss of smell	42 (54.5)	10 (52.6)
Fatigue	38 (49.4)	7 (36.8)
Malaise	6 (7.8)	1 (5.3)
Myalgias or body aches	34 (44.2)	8 (42.1)
Sore throat	12 (15.6)	1 (5.3)
Chills	25 (32.5)	6 (31.6)
Nasal congestion	6 (7.8)	0 (0)
Other	32 (41.6)	7 (36.8)
Duration of symptoms in days (median [range])	14 (1-43)	13 (6-30)
Days from symptom onset to positive SARS-CoV-2 PCR test (median [range])	6 (0-36)	6 (1-31)
Days from symptom onset to 1-month blood sample collection (median [range])	41 (21-84)	34 (22-71)
Hospitalization	6 (7.8)	1 (5.3)
COVID medications		
Hydroxychloroquine	2 (2.6)	0 (0)
Chloroquine	1 (1.3)	0 (0)
Azithromycin	14 (18.2)	6 (31.6)
Lopinavir/ritonavir	0 (0)	0 (0)
Remdesivir	0 (0)	0 (0)
Convalescent plasma	0 (0)	0 (0)
None	61 (79.2)	12 (63.2)
Other	2 (2.6)	1 (5.3)

Extended Data Table 3 | Symptoms and follow up samples (months 4–11) of convalescent individuals

	Month 4		Month 7		Month 11	
	Total N= 76 N (%)	**Bone marrow biopsy N=19 N (%)**	**Total N= 76 N (%)**	**Bone marrow biopsy N=18 N (%)**	**Total N= 42 N (%)**	**Bone marrow biopsy N=12 N (%)**
Days from positive SARS-CoV-2 PCR test to follow up visit (median [range])	125 (102-192)	117 (105-150)	222 (191-275)	213 (200-247)	308 (283-369)	303 (283-325)
Days from symptom onset to blood sample collection (median [range])	131 (106-193)	124 (108-155)	227 (194-277)	222 (205-253)	314 (288-373)	309 (297-343)
Any symptom present at follow up visit	25 (32.9)	8 (42.1)	33 (43)	10 (55.6)	20 (47.6)	6 (50)
Fever	0 (0)	0 (0)	2 (2.6)	0 (0)	1 (2.4)	0 (0)
Cough	1 (1.3)	1 (5.3)	0 (0)	0 (0)	1 (2.4)	0 (0)
Dyspnea	7 (9.2)	2 (10.5)	6 (7.9)	3 (16.7)	6 (14.3)	3 (25)
Nausea	1 (1.3)	0 (0)	1 (1.3)	0 (0)	0 (0)	0 (0)
Vomiting	1 (1.3)	1 (5.3)	0 (0)	0 (0)	0 (0)	0 (0)
Diarrhea	2 (2.6)	1 (5.3)	1 (1.3)	0 (0)	0 (0)	0 (0)
Headaches	1 (1.3)	0 (0)	3 (3.9)	0 (0)	2 (4.8)	0 (0)
Loss or altered taste	8 (10.5)	0 (0)	9 (11.8)	1 (5.6)	5 (11.9)	1 (8.3)
Loss or altered smell	13 (17.1)	2 (10.5)	12 (15.8)	2 (11.1)	8 (19)	2 (16.7)
Fatigue	9 (11.8)	4 (21.1)	13 (17.1)	5 (27.8)	8 (19)	3 (25)
Forgetfulness/brain fog	8 (10.5)	6 (31.6)	12 (15.8)	6 (33.3)	10 (23.8)	4 (33.3)
Hair loss	5 (6.6)	1 (5.3)	3 (3.9)	1 (5.6)	2 (4.8)	0 (0)
Other	7 (9.2)	3 (15.8)	12 (15.8)	1 (5.6)	10 (23.8)	1 (8.3)
Joint pain	3 (3.9)	1 (5.3)	7 (9.2)	1 (5.3)	3 (7.1)	0 (0)

Extended Data Table 4 | Healthy control demographics

Variable	Total N= 11 N (%)
Age (median [range])	38 (23-53)
Sex	
Female	3 (27.3)
Male	8 (72.7)
Race	
White	9 (71.8)
Black	1 (9.1)
Asian	1 (9.1)

nature research

Corresponding author(s): Ali H. Ellebedy

Last updated by author(s): May 26, 2021

Reporting Summary

Nature Research wishes to improve the reproducibility of the work that we publish. This form provides structure for consistency and transparency in reporting. For further information on Nature Research policies, see Authors & Referees and the Editorial Policy Checklist.

Statistics

For all statistical analyses, confirm that the following items are present in the figure legend, table legend, main text, or Methods section.

n/a	Confirmed	
☐	☒	The exact sample size (*n*) for each experimental group/condition, given as a discrete number and unit of measurement
☐	☒	A statement on whether measurements were taken from distinct samples or whether the same sample was measured repeatedly
☐	☒	The statistical test(s) used AND whether they are one- or two-sided *Only common tests should be described solely by name; describe more complex techniques in the Methods section.*
☒	☐	A description of all covariates tested
☐	☒	A description of any assumptions or corrections, such as tests of normality and adjustment for multiple comparisons
☐	☒	A full description of the statistical parameters including central tendency (e.g. means) or other basic estimates (e.g. regression coefficient) AND variation (e.g. standard deviation) or associated estimates of uncertainty (e.g. confidence intervals)
☐	☒	For null hypothesis testing, the test statistic (e.g. *F*, *t*, *r*) with confidence intervals, effect sizes, degrees of freedom and *P* value noted *Give P values as exact values whenever suitable.*
☒	☐	For Bayesian analysis, information on the choice of priors and Markov chain Monte Carlo settings
☒	☐	For hierarchical and complex designs, identification of the appropriate level for tests and full reporting of outcomes
☐	☒	Estimates of effect sizes (e.g. Cohen's *d*, Pearson's *r*), indicating how they were calculated

Our web collection on statistics for biologists contains articles on many of the points above.

Software and code

Policy information about availability of computer code

Data collection	Flow cytometry data were acquired using SpectroFlo software v2.2.
Data analysis	Flow cytometry data were analyzed using FlowJo v10 and Prism v8 ELISA and ELISpot data were analyzed using Prism v8 and SAS 9.4

For manuscripts utilizing custom algorithms or software that are central to the research but not yet described in published literature, software must be made available to editors/reviewers. We strongly encourage code deposition in a community repository (e.g. GitHub). See the Nature Research guidelines for submitting code & software for further information.

Data

Policy information about availability of data

All manuscripts must include a data availability statement. This statement should provide the following information, where applicable:

- Accession codes, unique identifiers, or web links for publicly available datasets
- A list of figures that have associated raw data
- A description of any restrictions on data availability

All relevant data are available from the corresponding author upon reasonable request.

Field-specific reporting

Please select the one below that is the best fit for your research. If you are not sure, read the appropriate sections before making your selection.

☒ Life sciences ☐ Behavioural & social sciences ☐ Ecological, evolutionary & environmental sciences

Life sciences study design

All studies must disclose on these points even when the disclosure is negative.

Sample size	No statistical methods were used to determine sample size. 77 convalescent patients and 11 control participants were enrolled based on recruitment; these numbers provided sufficient power to determine differences in SARS-CoV-2 responses between the groups.
Data exclusions	No data were excluded
Replication	Samples were collected from 77 convalescent patients and 11 control participants. ELISA for each participant at each timepoint was performed once with two technical replicates. ELISpot and flow cytometry experiments were performed once for each sample at each timepoint.
Randomization	Different experimental groups were not assigned.
Blinding	No blinding was done in this study; subjective measurements were not made.

Reporting for specific materials, systems and methods

We require information from authors about some types of materials, experimental systems and methods used in many studies. Here, indicate whether each material, system or method listed is relevant to your study. If you are not sure if a list item applies to your research, read the appropriate section before selecting a response.

Materials & experimental systems

n/a	Involved in the study
☐	☒ Antibodies
☐	☒ Eukaryotic cell lines
☒	☐ Palaeontology
☒	☐ Animals and other organisms
☐	☒ Human research participants
☒	☐ Clinical data

Methods

n/a	Involved in the study
☒	☐ ChIP-seq
☐	☒ Flow cytometry
☒	☐ MRI-based neuroimaging

Antibodies

Antibodies used	IgG-HRP (goat polyclonal, Jackson ImmuoResearch 109-035-088), IgG-BV480 (goat polyclonal, Jackson Immunoresearch 109-685-098), IgD-SB702 (IA6-2, Thermo 67-9868-42), IgA-FITC (M24A, Millipore CBL114F), CD45-A532 (HI30, Thermo 58-0459-42), CD38-BB700 (HIT2, BD Horizon 566445), Blimp1-A700 (646702, R&D IC36081N), CD20-Pacific Blue (2H7, 302320), CD4-BV570 (OKT4, 317445), CD24-BV605 (ML5, 311124), streptavidin-BV650 (405232), Ki-67-BV711 (Ki-67, 350516), CD19-BV750 (HIB19, 302262), CD19-PE (HIB19, 302254), CD71-PE (CY1G4, 334106), CXCR5-PE-Dazzle 594 (J252D4, 356928), CD27-PE-Cy7 (O323, 302838), CD71-PE-Cy7 (CY1G4, 334112), CD20-APC-Fire750 (2H7, 302358), IgM-APC-Fire750 (MHM-88, 314546), CD3-APC-Fire810 (SK7, 344858); all Biolegend.
Validation	Commercial antibodies were validated by their respective manufacturers per their associated data sheets and titrated in the lab for their respective assay (ELISA or flow cytometry) by serial dilution

Eukaryotic cell lines

Policy information about cell lines

Cell line source(s)	Expi293F (Thermo)
Authentication	The cell line was not authenticated
Mycoplasma contamination	Cell lines were not tested for mycoplasma contamination. Growth rates were consistent with manufacturer's published data.
Commonly misidentified lines (See ICLAC register)	No commonly misidentified cell lines were used

Human research participants

Policy information about studies involving human research participants

Population characteristics	77 SARS-CoV-2 convalescent study participants were recruited, ages 21-69, 49.4% female, 50.6% male 11 healthy control participants with no history of SARS-CoV-2 infection were recruited, ages 23-53, 27.3% female, 72.7% male
Recruitment	Study participants were recruited from the St. Louis metropolitan area by the Washington University Clinical Trials Unit. Potential self-selection and recruiting biases are unlikely to affect the parameters we measured.
Ethics oversight	The study was approved by the Washington University IRB

Note that full information on the approval of the study protocol must also be provided in the manuscript.

Flow Cytometry

Plots

Confirm that:

☒ The axis labels state the marker and fluorochrome used (e.g. CD4-FITC).

☒ The axis scales are clearly visible. Include numbers along axes only for bottom left plot of group (a 'group' is an analysis of identical markers).

☒ All plots are contour plots with outliers or pseudocolor plots.

☒ A numerical value for number of cells or percentage (with statistics) is provided.

Methodology

Sample preparation	Peripheral blood and bone marrow mononuclear cells were isolated from EDTA anticoagulated blood and bone marrow aspirates, respectively using density gradient centrifugation, and remaining RBCs were lysed with ammonium chloride lysis buffer. Bone marrow plasma cells were magnetically enriched from bone marrow mononuclear cells and immediately used for ELISpot or cryopreserved in 10% dimethylsufoxide in FBS for flow cytometric analysis. PBMCs were immediately used or cryopreserved in 10% DMSO in FBS.
Instrument	Cytek Aurora
Software	Flow cytometry data were acquired using Cytek SpectroFlo software, and analyzed using FlowJo (Treestar) v10.
Cell population abundance	Cells were not sorted
Gating strategy	Gating strategies are shown in extended data figure

☒ Tick this box to confirm that a figure exemplifying the gating strategy is provided in the Supplementary Information.